Published in final edited form as:
J Mol Cell Cardiol. 2020 February ; 139: 62–74. doi:10.1016/j.yjmcc.2020.01.005.

Age- and sex-dependent differences in extracellular matrix metabolism associate with cardiac functional and structural changes

Gabriel A. Grilo[a], **Patti R. Shaver**[a], **Hamilton J. Stoffel**[a], **Caleb Anthony Morrow**[a], **Octavious T. Johnson**[a], **Rugmani P. Iyer**[a], **Lisandra E. de Castro Brás**[a,b,*]

[a]Department of Physiology, The Brody School of Medicine, East Carolina University, Greenville, NC 27834, United States of America

[b]Department of Cardiovascular Sciences, The Brody School of Medicine, East Carolina University, Greenville, NC 27834, United States of America

Abstract

Age-related remodeling of the heart causes structural and functional changes in the left ventricle (LV) that are associated with a high index of morbidities and mortality worldwide. Some cardiac pathologies in the elderly population vary between genders revealing that cardiac remodeling during aging may be sex-dependent. Herein, we analyzed the effects of cardiac aging in male and female C57Bl/6 mice in four age groups, 3, 6, 12, and 18 month old (n = 6–12 animals/sex/age), to elucidate which age-related characteristics of LV remodeling are sex-specific. We focused particularly in parameters associated with age-dependent remodeling of the LV extracellular matrix (ECM) that are involved in collagen metabolism. LV function and anatomical structure were assessed both by conventional echocardiography and speckle tracking echocardiography (STE). We then measured ECM proteins that directly affect LV contractility and remodeling. All data were analyzed across ages and between sexes and were directly linked to LV functional changes. Echocardiography confirmed an age-dependent decrease in chamber volumes and LV internal diameters, indicative of concentric remodeling. As in humans, animals displayed preserved ejection fraction with age. Notably, changes to chamber dimensions and volumes were temporally distinct between sexes. Complementary to the traditional echocardiography, STE revealed that circumferential strain rate declined in 18 month old females, compared to younger animals, but not in males, suggesting STE as an earlier indicator for changes in cardiac function between sexes. Age-dependent collagen deposition and expression in the endocardium did not differ between sexes; however, other factors involved in collagen metabolism were sex-specific. Specifically, while decorin, osteopontin, Cthrc1, and Ddr1 expression were age-dependent but sex-independent, periostin, lysyl oxidase, and Mrc2 displayed age-dependent and sex-specific differences. Moreover, our data also suggest that with age males and females have distinct TGFβ signaling pathways. Overall, our results give evidence of sex-specific molecular changes during physiological cardiac remodeling that associate with age-dependent structural and functional

*Corresponding author at: The Brody School of Medicine, East Carolina University, 600 Moye Blvd., Mail stop 634, Greenville, NC 27834, United States of America. decastrobrasl14@ecu.edu (L.E. de Castro Brás).

Declaration of Competing Interest
None.

dysfunction. These data highlight the importance of including sex-differences analysis when studying cardiac aging.

Keywords

Aging; Cardiac dysfunction; Strain analysis; Collagen metabolism; Sex differences

1. Introduction

Independent of conventional risk factors (e.g. hypertension, smoking, and diabetes), physiological remodeling of the heart during natural aging is a major component for the development of cardiovascular diseases (CVD) and heart failure (HF) [1–3]. In the United States, recent statistical data evaluating aging and CVD report that: 1) There is a 145% increase in the number of deaths caused by CVD in patients between 65 and 85 years of age; 2) Mortality on individuals > 85 years old represents 40% of all CVD-related deaths [4]; and 3) HF prevalence rises from 2% in the general population to > 10% among people > 70years of age [5,6]. This occurs not only because aging prolongs exposure to several other cardiovascular risks, but also due to intrinsic cardiac aging. Intrinsic cardiac aging is defined by the following factors: an increase in left ventricular (LV) hypertrophy, as well as in atrial fibrillation; a slowly progressive age-dependent degeneration and decline in diastolic function, which reduces cardiac functional reserve, predisposes the heart to stress, and contributes to increased cardiovascular mortality in the elderly [7,8]; and preserved systolic function during rest that declines with physical activity [9].

Aging causes structural deterioration of the cardiac tissues that associates with deregulation of the extracellular matrix (ECM). In particular, collagen deposition (fibrosis) is a hallmark of age-dependent LV remodeling [10]. Myocardial fibrosis results from excessive deposition and accumulation of collagen in the cardiac walls; this leads to a progressive increase of ventricular stiffness with the overall effect of reduced contractility [10]. Changes to the cardiac ECM composition directly affect cardiac structure and function. For example, cardiovascular aging not only includes an increase on collagen content but also the fragmentation and rupture of elastin fibers in the arterial walls [11]. This causes reduced arterial resilience that appears to be directly related to the pathogenesis of cardiac fibrosis in older individuals [12]. Besides providing structural support, the cardiac ECM also acts as a scaffold for cardiac cells, such as cardiomyocytes, to provide anatomical support and facilitate cell-cell and cell-matrix interactions. With age, the continuous increase in mechanical load, due to hemodynamic stress and the consequent decrease of cardiac compliance, leads to hypertrophic changes in cardiomyocytes [13]. These structural modifications are irreversible and result in permanent changes in cardiac function.

Gender related differences in cardiac structure and function have been reported in several clinical studies [14–17]. Data suggest some CVDs are more prominent in men, while others are seen more frequently in women [15]. These observations emphasize the concept that intrinsic cardiac alterations are not only age-dependent, but also sex-dependent, and that as aging occurs sex differences can predispose the prognosis of some cardiac pathologies.

Rodent models of cardiac aging, particularly mouse models, are a valuable tool as their cardiac aging phenotypes closely recapitulate the phenotypes of human cardiac aging [18,19]. Moreover, unlike humans laboratory mice do not develop the traditional risk factors that affect cardiac function with age, meaning that functional changes are dependent on intrinsic aging. In addition, their brief lifespan provides the opportunity to utilize mice as aging models to study the molecular, cellular, and anatomical processes involved in the intrinsic cardiac aging process within a short time period [20]. Accordingly, murine models are highly useful to investigate the underlying mechanisms involved in age-dependent LV remodeling and the physiology of cardiac aging.

In the last decades, conventional echocardiography has been routinely used in aging studies to analyze changes in cardiac structure and function both in humans and animal models [21]. More recently, strain analysis (also known as speckle tracking echocardiography, STE) emerged as a novel technique used for the assessment of LV global and segmental wall motion [22]. While strain determines how much the myocardium has deformed, strain rate indicates how fast the myocardium is deforming. This method identifies both regional and global systolic and diastolic LV function based on changes in the LV contractility [23]. STE is a recent, highly sensitive, and reproducible method that has been showed to be favorable for the examination of cardiac diseases and it is being used as a tool for the early detection of heart failure [24]. This non-invasive technique has also been used in the examination of myocardial function in translational research [25], and STE measurements further extend the quantitative parameters of conventional echocardiography.

In the present study, we had two main goals: 1) investigate sex-specific differences in cardiac ECM remodeling that occur in an age-dependent matter and 2) determine whether STE is a more sensitive tool, compared to conventional echocardiography, to identify earlier cardiac functional changes that are both sex- and age-dependent.

2. Materials and methods

2.1. Animals

Animal procedures were performed according to the “Guide for the Care and Use of Laboratory Animals” (NIH Notice Number: NOT-OD-12-020) and were approved by the Institutional Animal Care and Use Committee at the East Carolina University. Both male and female C57BL/6 mice (Charles River stock #027) were used in this study (n = 6–12/sex/age). Animals were bred in-house in the fully accredited animal facility at ECU managed by the Department of Comparative Medicine. Animals were housed at a controlled temperature (22 ± 2 °C) on a 12 h light/dark cycle, fed standard laboratory mice chow ad libitum, and had free access to tap water. Four age groups were analyzed: young (3–3.5 month old, m.o.), adult (6–6.5 m.o.), middle-aged (12–12.5 m.o.), and old (18–18.5 m.o.).

2.2. Conventional and speckle tracking echocardiography

Transthoracic echocardiography was performed using a Vevo 2100™ system (VisualSonics) with a 30 MHz image transducer (MS400). Mice were anesthetized with 1–2% isoflurane in an oxygen mix and hair was removed from the chest. Mice were placed on a supine position

on a heated platform with embedded electrocardiogram (ECG) leads. The body temperature and heart rate were monitored throughout the imaging procedure. Core body temperature was maintained at 37 °C and all images were acquired at heart rates > 400 bpm to achieve physiologically relevant measurements. Measurements were taken from the LV parasternal long axis (B-mode) and short axis (M-mode) views. For conventional echocardiography, three images of the parasternal long axis B-Mode were used to delineate the LV trace in full diastole (see Fig. 1E) and its consecutive full systole to obtain the averaged measurements of heart rate (HR), end-diastolic volume (EDV), end-systolic volume (ESV), stroke volume (SV), ejection fraction (EF), and cardiac output (CO) using the VevoLab 1.7.1 software. The wall thickness (anterior, AW; posterior, PW) and internal diameter (ID) of the LV were measured using three consecutive cardiac cycles in short-axis M-Mode (see Fig. 1E) that were averaged to evaluate LVAW;d, LVAW;s, LVID;d, LVID;s, LVPW;d and LVPW;s by the same methods as we previously described [26–32]. Fractional shortening (FS) and EF were calculated using the Vevo Lab 1.7.1 software algorithms. For STE, tracing of the cardiac wall was performed using 2D grayscale echocardiographic films of parasternal long and short axis views with a frame rate above 200 frames per second. Image depth, width, and gain settings were optimized to improve image quality. Images in B-mode displaying clear visualization of the LV endocardial border of both axes were selected and 3 successive cardiac cycles were chosen to delineate the myocardium by tracing the endocardial margin with an adjusted epicardial border. The long axis view was used to determine the longitudinal and radial peaks, while the short axis provided the respective radial and circumferential peaks. Measurements of the peaks of strain, strain rate, displacement, and velocity were calculated using the algorithm from VevoStrain™ (VisualSonics). The cardiac wall was separated in 6 distinct anatomical segments (anterior base, anterior middle, anterior apex, posterior apex, posterior middle, and posterior base) to determine regional strain parameters, and the average of these segments defined the global longitudinal, radial, and circumferential strain values. All echocardiographic readings/measurements were performed by one blinded individual to avoid technical variation and interpretation bias.

2.3. Collagen turnover

Collagen ELISA assays using plasma were performed using LSBio Mouse CTX/Collagen C-Terminal Telopeptide (Cat. # LS-F21349) and LSBio Mouse Procollagen I C-Terminal Propeptide (Cat. #LS-F14803). Samples from groups 6, 12, and 18 m.o. (n = 6 each) were diluted 1:10, and assays were performed per manufacturer's instructions.

2.4. Histological quantification of collagen, elastin, and myocyte cross-sectional area

Image acquisition was obtained with an Olympus BX51 Microscope (Olympus, Pennsylvania) and CellSens V1.7 software (Olympus, Pennsylvania). For each LV, one image was taken at 4×, and a minimum of five images were taken at 40×. The picro-sirius red (PSR, collagen) and Miller's elastin positive stain were then quantified utilizing Image-Pro Premier Offline 9.1 Software (Media Cybernetics, Maryland). The 40× images of each animal were quantified based on total collagen or elastin positive area (βm^2) per field of view and averaged. Myocyte cross-sectional analysis was completed using the same images and software that were used for PSR collagen analysis and quantification. Only images that showed distinct cross-sections of cardiomyocytes were used, with a minimum of 10

myocytes measured per animal. The average cardiomyocyte cross-sectional area (βm^2) was calculated for each animal and compared among groups.

2.5. Protein quantification

LV proteins were extracted by Protein Extraction Reagent Type 4 (Sigma, C0356) with 1× Protease Inhibitors (Roche, #11836153001) as described previously [33]. Due to the large number of groups, samples were randomized for protein extraction to avoid experiment-dependent bias and ensure reproducibility across groups. The Bradford assay was used for protein quantification with IgG serving as standards. Immunoblots against collagen 1, collagen 3, decorin, lysyl oxidase, periostin, osteopontin, Smad2/3, pSmad2/3, ERK1/2, pERK1/2, TGFβ1, TGFβRI, and TGFβRII were performed using the following antibodies and dilutions: Collagen I alpha 1 1:1000 (Novusbio, NBP2-29651), Collagen III alpha 1/COL3A1 1:1000 (Novusbio NBP2–15946), Decorin 1:2000 (R&D Systems, AF1060), Lysyl oxidase 1:2000 (LOX, Novusbio, NBP1–74065), Periostin1:6000 (R&D Systems, AF2955), Osteopontin 1:2000 (OPN, R&D Systems, AF808), Smad2/3 1:125 (R&D Systems, AF3797-SP), pSmad2/3 [p Ser465, p Ser467] 1:4000 (Novusbio, NBP2–44217), ERK1/2 1:5000 (Novusbio, NBP2–67378), pERK1/2 [Thr185, Tyr187] 1:1000 (Thermo, 44–680-G), TGFβ1 1:500 (Thermo, MA5–15065), TGFβR1 1:1000 (Thermo, MAB5871) and TGFβRII 1:500 (Thermo, AF532). Ten μg of total protein was loaded per well (n = 4/sex/age; groups 6, 12, and 18 m.o.) and visualized with Pierce reversible membrane protein stain kit to ensure equal loading and extraction reproducibility. Image acquisition was performed using a UVP ChemiDoc-It TS2 Imager. Densitometry was performed using UVP software and values were normalized to total loaded protein.

2.6. RNA extraction and cDNA amplification

RNA was obtained to determine whether age- and sex-dependent changes were present either at the transcription or translation level. Total RNA was extracted using TRIzol and the Pure Link RNA mini kit (Ambion, 12183018A) according to manufacturer's instructions. RNA was treated with ezDNAse (Invitrogen) and reverse-transcribed into cDNA using the High capacity RNA to cDNA kit (Applied Biosystems) according to the manufacturer's instructions.

2.7. Aging and extracellular matrix remodeling gene arrays

Custom gene arrays for aging pathways (24 genes,3 housekeeping genes, genomic DNA control, reverse transcription control, and positive control) and factors involved in extracellular matrix remodeling (84 genes, 5 housekeeping genes, and controls) were purchased (Qiagen) and performed using the QuantStudio Flex 6 (Applied Biosystems). Values were expressed as $2^{-\Delta Ct}$.

2.8. Statistical analysis

Power analysis was used to determine group sizes (GraphPad StatMate 2) based on previous data from our lab and others. Data are reported as mean ± SD, outliers were identified using the Grubbs method with an alpha set at 0.05 [34]. Outliers were included when it did not affect the final statistical result; when the outlier affected overall results this was noted

on the results section and the final statistical analysis was presented with and without the outlier. Comparisons between groups were performed using one-way ANOVA followed by the Student-Newman-Keuls post hoc test when the Bartlett's variation test passed or using the nonparametric Kruskal-Wallis test followed by Dunn post hoc test when the Bartlett's variation test did not pass. A $p < .05$ was considered significant (GraphPad InStat 3).

3. Results and discussion

3.1. C57Bl/6 mice as a model of age-dependent cardiac dysfunction

A large body of evidence has firmly established the laboratory mouse as an excellent model of human aging [35–38]. As the mouse has a relatively short lifespan it allows for aging studies to proceed in a reasonable amount of time. Additionally, environmental factors that affect aging can be easily controlled [39]. In this study we used C57Bl/6 mice as a model of cardiac aging. All conventional echocardiography data was normalized according to the methods described by Hagdorn et al. [40] Shortly, one-dimensional measures (i.e. length) were indexed to body weight $(BW)^{1/3}$, and three-dimensional measures (i.e. volumes and mass) to BW. As in humans, we observed reduction in chamber volumes in the older animals (18 m.o.) compared to all other ages, seen as decreased end-diastolic (EDV) and end-systolic (ESV) volumes (Table 1). In accordance with these data, LV internal diameters in diastole and systole (LV IDd and LV IDs) were reduced in the old animals compared to the younger groups, suggestive of concentric remodeling. This was concomitant with preserved ejection fraction and, therefore, preserved systolic function in the adult, middle-age, and old animals. HF with preserved ejection fraction (HFpEF) is a hallmark of age-dependent cardiac dysfunction in humans [41,42]. Of note, while EF and fractional shortening (FS) did not decline after 6 months of age, young adults (3 m.o. group) displayed higher EF and FS compared to other ages. Several reports have shown that EF and stroke volume (SV) are higher in adolescence compared to adults; it was proposed that this was a result of increased growth hormones and physical activity in adolescents [42,43]. We also observed higher SV in the young adults compared to middle-age and old groups ($p < .05$).

Contrarily to systolic function, a decline in diastolic function is a key characteristic of cardiac aging [44,45]. While active relaxation is reduced due to age-associated decreases in sarcoplasmic reticulum calcium uptake [46,47], passive stiffness can significantly contribute to the impaired diastolic function [48,49]. As mentioned above, we observed an age-dependent reduction in volumes and dimensions, representative of decreased relaxation and increased concentric remodeling. Overall, our results demonstrate that C57Bl/6 mice are an excellent tool to study age-dependent cardiac remodeling and dysfunction as the model mimics human aging.

3.2. Sex-dependent differences in concentric remodeling and hypertrophy

The age-dependent differences observed in SV were driven only by males. While middle-age and old males displayed reduced SV ($p < .05$) compared to young adults, females did not present SV differences with age (Fig. 1A). As expected, age-dependent decrease to chamber volumes were mostly observed in males (EDV: $p < .05$ 18 m.o. versus 3 m.o.; ESV: $p < .05$ 18 m.o. versus all other ages), while females displayed reduced ESV and EDV only

at 18 months compared to 12 m.o. animals. These results are suggestive of earlier concentric remodeling in males (Fig. 1B and C). Similarly, while old males presented reduced LV IDd and LV IDs compared to all other groups, old females only showed changes when compared to the middle-aged (12 m.o.) group. Other labs have reported the reproductive senescent phase of female mice to occur between 9 and 12 m.o [50–52]. It is possible that the drastic cardiac changes we are observing in 18 m.o. females, compared to 12 m.o., are a result of established reproductive senescence. Measurements of posterior (LVPW) and anterior (LVAW) wall thicknesses were sex-independent. Overall, these data indicate that LV remodeling occurs at a later stage in females compared to males and/or the remodeling rate is slower in females. To further analyze sex-related differences in LV function with age, we plotted EDV and ESV values stratified by sex to visualize the volume regulation graph, as proposed recently by Kerkhof and coworkers as a means of analyzing LV pump function, independent of afterload variations [53]. The regression lines for males and females did not differ significantly between sexes, although males presented higher linearity fit ($R^2 = 0.82$ in males versus 0.53 in females, Fig. 2). Importantly, data plotted was age-matched and both females and males presented significant EDV and ESV relationship in an age-dependent manner ($p < .0001$ for both sexes).

Detailed studies that report sex-differences in physiological cardiac aging in animal models are rather scarce. We compared our data to that of others and found both similarities [25,54], as well as critical differences, mainly due to the strain and age of the animals when the echocardiography was acquired. For example, Koch et al. analyzed cardiac function in both male and female FVB/N mice from 3 to 16 months of age [55]. On their study they observed both reduced systolic and diastolic function in males but not in females. This difference could be a result of the animal strain used, as well as the age of the animals; particularly, since for females we mostly observed cardiac changes only between the 12 m.o. and 18 m.o. groups. Several manuscripts on age-related changes in cardiac function report decreasing diastolic and systolic function beginning as early as 12 m.o. of age; however, those reports did not track gender differences [56–59]. When we combined all data, independent of sex, EDV, ESV, IDd, and IDs were all significantly reduced in the old mice (18 m.o.) compared to all other groups, suggestive of cardiac remodeling and hypertrophy. Indeed, the cross-section areas of cardiomyocytes were significantly higher at 18 m.o. compared to all other ages (Fig. 3), and this was independent of sex. Age-related cardiomyocyte loss can increase the mechanical burden on the surviving cardiomyocytes and lead to compensatory hypertrophy [60]. Morphometric analysis in humans suggest that the volume of LV cardiomyocytes increases with age and that this is more pronounced in men than in women [61,62]. Nonetheless, whether age-dependent cardiomyocyte loss and hypertrophy occur at different rates and through different mechanisms in male and female hearts has not been established, and additional studies are necessary to answer this question. In our mouse model, we did not observe a histological difference in cardiomyocyte hypertrophy between males and females. This raised the question whether males and females displayed differences in age-dependent ECM secretion and remodeling that could explain the age-dependent reduced chamber volumes.

3.3. Left ventricular loss of contractility

Two-dimensional STE enabled us to assess myocardial strain, i.e. deformation resulting from changes in length. Strain analysis is a derivative of Doppler imaging and has been reported to be a more direct measurement of intrinsic myocardial contractility than global values such as EF or FS [23,63]. While a positive strain value indicates elongation of tissue, a negative strain value indicates shortening of tissue. Longitudinal strain (long axis) analysis revealed higher strain rate (rate of strain change over time) at 6 and 12 m.o., compared to the young 3 m.o. group and this change was only observed in females (Fig. 4A). These data were similar to what we observed with conventional echocardiography (see Table 1). We also measured radial strain, both in the long and short axes. Both global radial strain and strain rate displayed an age-dependent increase trend, but this did not reach significant values. Finally, analysis of circumferential strain (short axis) revealed the 18 m.o. group displayed increased velocity and reduced strain rate compared to all other ages (Fig. 4B), giving evidence of increased strain deformation in the older animals. For both of these datasets, one outlier was identified and removed in the 6 month group [including outlier $p < .05$ 6 × 18 and 12 × 18; excluding outlier $p < .05$ 3 × 18, 6 × 18, and 12 × 18]. Increased circumferential strain displacement was also observed in the 18 m.o. group compared to 12 m.o. Interestingly, all circumferential changes were driven by females, while males did not display any age-dependent significant changes. This suggests STE allows for earlier detection of age-dependent and sex-specific cardiac changes. Several studies support STE measurements as a more sensitive and informative technique regarding cardiac contractility [25,64]. Shah and colleagues showed that impaired longitudinal strain could represent a novel imaging biomarker to identify patients with heart failure and preserved EF, since STE allowed for identification of impaired systolic function even when EF seemed normal [65]. In our study, STE confirmed what we observed with conventional echocardiography and further allowed to identify age-dependent strain changes in females.

3.4. Sex-specific regulation of cardiac collagen pathway and metabolism

To determine changes in myocardial matrix composition that could explain the changes observed in cardiac contractility, chamber volumes, and concentric remodeling, we first assessed total levels of LV elastin and collagen both by histological analysis and by protein expression. No significant changes were observed in elastin levels independent of sex or age. Nonetheless, a trend for an age-dependent decrease in elastin was observed, which would be expected and match the age-dependent loss of contractility. We quantified the area of interstitial collagen in the LV using PSR staining. The histological analysis showed that old, 18 m.o., mice displayed significant interstitial myocardial fibrosis compared to younger mice (Fig. 5A). This increase in fibrosis is a sign of myocardial stiffness that leads to impaired relaxation and, therefore, diastolic dysfunction. This was confirmed by immunoblot quantification of collagen type 1 (Fig. 5B, $n = 4$/sex/age). Age-dependent fibrosis did not differ between sexes. We also quantified collagen type 3 to assess levels of turnover, but no differences were observed independent of age or sex (Fig. 5B). Finally, we assessed levels of collagen turnover in plasma. For homeostasis, a healthy heart needs to maintain a balance between collagen synthesis and degradation (i.e. collagen turnover). Myocardial fibrosis, including age-dependent fibrosis, can result from an imbalance between the dynamics of collagen metabolism that leads to increased synthesis (deposition) of

collagen I and III with reduced or unchanged collagen degradation. As a marker of collagen synthesis, we quantified the circulatory levels of the procollagen I C-terminal propeptide (PICP); additionally, the collagen I C-Terminal telopeptide (CITP) was measured as a marker of collagen degradation [66]. Plasma levels of PICP were similar among ages; however, we observed reduced collagen degradation at 12 and 18 m.o. visualized by reduced levels of CITP (Fig. 5C). These data are in accordance with the observed interstitial collagen deposition and protein expression in these age groups. The onset of age-dependent cardiac stiffness is likely a result of increased cardiac ECM remodeling, in particular, a shift in the collagen turnover pathway towards decreased degradation resulting in an overall increase in collagen levels. To further test this hypothesis, we investigated changes in the canonic transforming growth factor (TGF)-β pathway. TGFβ1 expression in males was not different with age; however, females presented enhanced TGFβ1 expression ($p < .05$, Fig. 6A). We then looked at TGFβ receptor (TGFβR) levels; as observed with the ligand, TGFβR1 was increased only in females and this increase was age dependent (Fig. 6B). No differences were noted on TGFβR2 for either sex. Smad2/3 was again increased in an age-dependent manner only in females (Fig. 6C) and pSmad2/3 was increased in both males and females in the 18 m.o. animals. The ratio pSmad/Smad was not different with age in the females but was increased in both 12 and 18 m.o. males ($p < .05$ versus 6 m.o.). Since we did not observe an increase in either TGFβ1 and TGFβR1 in males with age, we did not expect to see increased pSmad2/3 However several labs have reported that the linker region of nuclear localized Smads can undergo phosphorylation by extracellular signal regulated kinase (Erk) and c-Jun N-terminal kinase (JNK) [67–70]. This suggests that even though both male and females display age-dependent cardiac fibrosis the underlying pathways may be distinct.

Using immunoblotting, we further looked at proteoglycans and proteins known to be involved in collagen deposition and maturation that could participate in sex-specific fibrosis (Fig. 7). Decorin, a small leucine-rich proteoglycan, has been implicated in the regulation of fibrillogenesis [71]. Similar to the observations from collagen type 1, decorin levels increased in both sexes at 18 m.o. ($p < .05$ versus all other ages). Decorin has previously been reported to directly affect collagen structure, particularly, decorin deficiency results in mice with fragile skin, abnormal tendons, and fundamental alterations in collagen fibers [72].

Lysyl oxidase (LOX), necessary for collagen fibril crosslinking, and periostin, a matricellular protein, showed sex-dependent data. Specifically, an age-dependent increase in LOX was only present in females and periostin was increased in males only ($p < .05$ at 18 m.o. versus all other ages). An increase in LOX in old mice supports the observed reduction in cardiac contractility since higher levels of collagen crosslinking imply increased LV stiffness. Reports have shown periostin to associate with levels of fibrosis in failing hearts [73]. In addition, excessive periostin expression in old rat hearts (24 m.o.) has been shown to contribute to cardiomyocyte senescence [74], implicating periostin in age-dependent cardiac fibrosis and dysfunction.

Osteopontin (OPN), a phosphorylated glycoprotein that exists as an immobilized matrix protein and as a cytokine [75], was also overexpressed in both sexes at 18 m.o. compared to younger ages. OPN is secreted by several cell types including fibroblasts and macrophages

[76,77]. OPN is involved in a variety of biological processes, such as chemotaxis, adhesion support, cell survival, and wound repair [78]. In the healthy myocardium, OPN levels are negligible, but it is robustly expressed under pathological conditions [79]. Moreover, OPN cardiac expression is associated with consecutive development of extensive fibrosis, LV stiffness, and systolic dysfunction [80,81]. Our results are in accordance with this notion, both collagen type 1 (fibrosis) and OPN displayed an age-dependent increase in the LV, particularly at 18 m.o. This coincided with reduced LV chamber volumes.

Using gene array analysis, we assessed expression of 84 extracellular matrix proteins and adhesion molecules that may be involved in LV structural changes. In accordance with what we observed by collagen quantification, the collagen triple helix repeat-containing protein 1 (Cthrc1), a negative regulator of collagen deposition, was robustly decreased both at 12 and 18 m.o. in both sexes (Fig. 8). The discoidin domain receptor 1 (Ddr1) displayed an age-dependent decrease both in females and males. Ddr1 is a cell surface tyrosine kinase receptor for fibrillar collagen and regulates cell attachment to the extracellular matrix (ECM) and remodeling of the ECM by up-regulation of matrix metalloproteinases (MMPs) [82–84]. The C-type mannose receptor 2 (Mrc2), which deficiency leads to fibrosis as a result of reduced collagen uptake, was also reduced at 18 m.o. compared to younger groups; however, this reduction was driven by females. Overall, our results point to an age-dependent dysregulation of collagen metabolism that, with time, leads to cardiac fibrosis.

3.5. Cardiac homeostasis with age

Genes involved in cardiac homeostasis, such as the atrial natriuretic peptide A (Nppa), the receptor atrial natriuretic peptide receptor 1 (Npr1), and ubiquitin B (Ubb), were all reduced with age, particularly at 18 m.o. (Fig. 9). Of these, only Npr1 changes were driven by females, whereas Nppa and Ubb expression were sex independent. The cardiac hormone natriuretic peptide A (ANP), and its receptor Npr1, play a key role in cardiovascular homeostasis through regulation of natriuresis, diuresis, and vasodilation [85]. ANP is also anti-hypertrophic in the heart, which is independent of its systemic blood pressure-lowering effect. Studies using Nppa and Npr1 knockout mice, demonstrated that while dietary or pharmacological treatments lowered blood pressure, they did not prevent cardiac hypertrophy [86,87]. Additionally, cardiac-specific Npr1 knockout mice display normal blood pressure but exhibit marked cardiac hypertrophy [88]. When we plotted these markers of cardiac homeostasis against cardiomyocyte cross-sectional area (paired values), even though regression lines slopes were not different between sexes, females homeostasis significantly associated with myocyte area ($p < .05$ for all markers). Taken together, our results strongly suggest a link between age-dependent loss of cardiac homeostasis in females and cardiac hypertrophy.

4. Study limitations and perspectives

The use of a mouse aging model comes with inherent limitations. First, we recognize that older mice don’t develop the same age-related cardiovascular pathologies (ex. atherosclerosis) as elderly humans that associate with differences in cardiac function. While this limits clinical significance, it has the advantage of allowing us to isolate only

age-specific changes. Second, we used 18 m.o. C57Bl/6 as the eldest group in our study, which is on the lower range for animals typically termed as old. Aging studies commonly refer to C57Bl mice > 17–32 m.o. as being “old”; however, some studies will term animals > 24 m.o. as senescent [89–92]. Nonetheless, it is feasible to surmise that the structural and functional changes observed at the investigated ages will be maintained with increasing age.

5. Conclusions

The purpose of this study was two-fold, first determine whether STE analysis could provide further insight in age-dependent and sex-dependent loss of cardiac contractility and function; and second, evaluate whether cardiac ECM remodeling with age evokes structural changes that differ between females and males.

Changes in conventional echocardiographic systolic indices, such as EF and FS, commonly manifest late in progressive cardiac disease and may not be sensitive enough to reveal subtle changes in the LV structure and global function. Thus, in this study we investigated whether functional changes in age-dependent cardiac remodeling could be earlier detected by STE analysis. Here the goal was to provide further insight into age- and sex-dependent loss of cardiac contractility and function. We found that both conventional echocardiography and STE provided evidence of age-related loss of contractility with preserved systolic function. However, STE allowed for the detection of sex-specific cardiac changes at an earlier life stage compared to traditional echocardiographic methods. By conventional echocardiography, most significant changes observed in LV chamber dimensions in females occurred between 12 and 18 months of age (e.g. EDV, ESV, IDd, IDs; Table 1). While males displayed a progressive decline with the 18 m.o. group showing reduced dimensions compared to all other ages. It is possible that the drastic cardiac changes we are observing in 18 m.o. females, compared to 12 m.o., are a result of established reproductive senescence. Noteworthy, measurements of STE indicated that female mice, but not males, present a significant deterioration in all circumferential strain modes in the 18 m.o. group compared to both the 6 and 12 m.o. animals.

We then focused on ECM components that could induce cardiac structural changes involved in reduced contractility, such as fibrillar collagen. We did not observe sex-differences in age-dependent deposition of cardiac collagen, a hallmark of cardiac physiological aging. Nonetheless, when we investigated other molecules involved in collagen metabolism, such as decorin, LOX, periostin, OPN, Cthrc1, Mrc2, and Ddr1, changes with age were sex-specific for periostin, LOX and Mrc2. While changes in periostin were present only in males, females presented age-dependent changes both in LOX and Mrc2. An increase in LOX affects collagen arrangement and crosslinking resulting in reduced contractility triggering concentric remodeling, which can associate with the robust differences observed in the functional parameters in the old females. Additionally, when we looked at the TGFβ canonic pathway, we also observed the highest age-dependent increases in females. Notably, our results provide evidence that 1) structural proteins such as periostin and LOX (essential for collagen maturation and crosslinking) are both age-dependent and sex-specific and 2) physiological fibrosis in males and females may have distinct fibrotic pathways. These data highlight the notion that physiological LV remodeling is more complex and involve more

processes beyond collagen deposition; several factors participate in collagen metabolism – from expression, to deposition, alignment, and maturation – and these are age- and sex-specific.

In summary, STE allows for early detection of functional changes and LV remodeling with age is distinct between sexes. In particular, male mice appear to present progressive changes in cardiac structure and function, while females present drastic structural changes between 12 and 18 m.o.

Acknowledgments

We acknowledge the technical contribution of Kylie R. Kennedy and Valentine Okafor. We acknowledge funding support from the East Carolina University (US) and the American Heart Association (US) [grant number 18AIREA33960311 and 19PRE34450066].

References

[1]. Strait JB, Lakatta EG, Aging-associated cardiovascular changes and their relationship to heart failure, Heart Fail. Clin 8 (1) (2012) 143–164. [PubMed: 22108734]

[2]. Oxenham H, Sharpe N, Cardiovascular aging and heart failure, Eur. J. Heart Fail 5 (4) (2003) 427–434. [PubMed: 12921803]

[3]. Sessions AO, Engler AJ, Mechanical regulation of cardiac aging in model systems, Circ. Res 118 (10) (2016) 1553–1562. [PubMed: 27174949]

[4]. Benjamin EJ, Virani SS, Callaway CW, Chamberlain AM, Chang AR, Cheng S, Chiuve SE, Cushman M, Delling FN, Deo R, de Ferranti SD, Ferguson JF, Fornage M, Gillespie C, Isasi CR, Jimenez MC, Jordan LC, Judd SE, Lackland D, Lichtman JH, Lisabeth L, Liu S, Longenecker CT, Lutsey PL, Mackey JS, Matchar DB, Matsushita K, Mussolino ME, Nasir K, O'Flaherty M, Palaniappan LP, Pandey A, Pandey DK, Reeves MJ, Ritchey MD, Rodriguez CJ, Roth GA, Rosamond WD, Sampson UKA, Satou GM, Shah SH, Spartano NL, Tirschwell DL, Tsao CW, Voeks JH, Willey JZ, Wilkins JT, Wu JH, Alger HM, Wong SS, Muntner P, Heart disease and stroke statistics-2018 update: a report from the American Heart Association, Circulation 137 (12) (2018) e67–e492. [PubMed: 29386200]

[5]. Komajda M, Hanon O, Hochadel M, Lopez-Sendon JL, Follath F, Ponikowski P, Harjola VP, Drexler H, Dickstein K, Tavazzi L, Nieminen M, Contemporary management of octogenarians hospitalized for heart failure in Europe: euro heart failure survey II, Eur. Heart J 30 (4) (2009) 478–486. [PubMed: 19106198]

[6]. Ponikowski P, Voors AA, Anker SD, Bueno H, Cleland JGF, Coats AJS, Falk V, Gonzalez-Juanatey JR, Harjola VP, Jankowska EA, Jessup M, Linde C, Nihoyannopoulos P, Parissis JT, Pieske B, Riley JP, Rosano GMC, Ruilope LM, Ruschitzka F, Rutten FH, van der Meer P, 2016 ESC guidelines for the diagnosis and treatment of acute and chronic heart failure: the task force for the diagnosis and treatment of acute and chronic heart failure of the European Society of Cardiology (ESC)developed with the special contribution of the heart failure association (HFA) of the ESC, Eur. Heart J 37 (27) (2016) 2129–2200. [PubMed: 27206819]

[7]. Dai D-F, Rabinovitch PS, Cardiac aging in mice and humans: the role of mitochondrial oxidative stress, Trends Cardiovasc. Med 19 (7) (2009) 213–220. [PubMed: 20382344]

[8]. Dai D-F, Chen T, Johnson SC, Szeto H, Rabinovitch PS, Cardiac aging: from molecular mechanisms to significance in human health and disease, Antioxid. Redox Signal 16 (12) (2012) 1492–1526. [PubMed: 22229339]

[9]. Lakatta EG, Levy D, Arterial and cardiac aging: major shareholders in cardiovascular disease enterprises: part II: the aging heart in health: links to heart disease, Circulation 107 (2) (2003) 346–354. [PubMed: 12538439]

[10]. Biernacka A, Frangogiannis NG, Aging and cardiac fibrosis, Aging Dis. 2 (2) (2011) 158–173. [PubMed: 21837283]

[11]. Duca L, Blaise S, Romier B, Laffargue M, Gayral S, El Btaouri H, Kawecki C, Guillot A, Martiny L, Debelle L, Maurice P, Matrix ageing and vascular impacts: focus on elastin fragmentation, Cardiovasc. Res 110 (3) (2016) 298–308. [PubMed: 27009176]

[12]. Pagoulatou S, Stergiopulos N, Evolution of aortic pressure during normal ageing: a model-based study, PLoS One 12 (7) (2017) e0182173. [PubMed: 28753657]

[13]. Chiao YA, Rabinovitch PS, The aging heart, Cold Spring Harbor Perspect. Med 5 (9) (2015) a025148.

[14]. Claessens TE, Rietzschel ER, De Buyzere ML, De Bacquer D, De Backer G, Gillebert TC, Verdonck PR, Segers P, Noninvasive assessment of left ventricular and myocardial contractility in middle-aged men and women: disparate evolution above the age of 50? Am. J. Physiol. Heart Circ. Physiol 292 (2) (2007) H856–H865. [PubMed: 17287452]

[15]. Kane AE, Howlett SE, Differences in cardiovascular aging in men and women, Adv. Exp. Med. Biol 1065 (2018) 389–411. [PubMed: 30051398]

[16]. Kerkhof PLM, Peace RA, Heyndrickx GR, Meijboom LJ, Sprengers RW, Handly N, Heart function analysis in cardiac patients with focus on sex-specific aspects, Adv. Exp. Med. Biol 1065 (2018) 361–377. [PubMed: 30051396]

[17]. Heinen A, Behmenburg F, Aytulun A, Dierkes M, Zerbin L, Kaisers W, Schaefer M, Meyer-Treschan T, Feit S, Bauer I, Hollmann MW, Huhn R, The release of cardioprotective humoral factors after remote ischemic preconditioning in humans is age- and sex-dependent, J. Transl. Med 16 (1) (2018) 112. [PubMed: 29703217]

[18]. Lakatta EG, Levy D, Arterial and cardiac aging: major shareholders in cardiovascular disease enterprises: part I: aging arteries: a “set up” for vascular disease, Circulation 107 (1) (2003) 139–146. [PubMed: 12515756]

[19]. Barger JL, Kayo T, Vann JM, Arias EB, Wang J, Hacker TA, Wang Y, Raederstorff D, Morrow JD, Leeuwenburgh C, Allison DB, Saupe KW, Cartee GD, Weindruch R, Prolla TA, A low dose of dietary resveratrol partially mimics caloric restriction and retards aging parameters in mice, PLoS One 3 (6) (2008) e2264. [PubMed: 18523577]

[20]. Gorbunova V, Bozzella MJ, Seluanov A, Rodents for comparative aging studies: from mice to beavers, Age (Dordr.) 30 (2–3) (2008) 111–119. [PubMed: 19424861]

[21]. Scherrer-Crosbie M, Thibault HB, Echocardiography in translational research: of mice and men, J. Am. Soc. Echocardiogr 21 (10) (2008) 1083–1092. [PubMed: 18723318]

[22]. Gao S, Ho D, Vatner DE, Vatner SF, Echocardiography in mice, Curr. Protoc. Mouse Biol 1 (2011) 71–83. [PubMed: 21743841]

[23]. An X, Wang J, Li H, Lu Z, Bai Y, Xiao H, Zhang Y, Song Y, Speckle tracking based strain analysis is sensitive for early detection of pathological cardiac hypertrophy, PLoS One 11 (2) (2016) e0149155. [PubMed: 26871457]

[24]. Smith PM, Daruwalla V, Freed BH, Spottiswoode BS, Kalisz K, Carr JC, Collins JD, Myocardial strain analysis in patients with heart failure with preserved ejection fraction using bright blood cine MR images: a comparison with speckletracking echocardiography, J. Cardiovasc. Magn. Reson 16 (Suppl. 1) (2014) P71.

[25]. de Lucia C, Wallner M, Eaton DM, Zhao H, Houser SR, Koch WJ, Echocardiographic strain analysis for the early detection of left ventricular systolic/diastolic dysfunction and dyssynchrony in a mouse model of physiological aging, J. Gerontol. A Biol. Sci. Med. Sci 74 (4) (2019) 455–461. [PubMed: 29917053]

[26]. de Castro Bras LE, Toba H, Baicu CF, Zile MR, Weintraub ST, Lindsey ML, Bradshaw AD, Age and SPARC change the extracellular matrix composition of the left ventricle, Biomed. Res. Int (2014) 810562 (2014). [PubMed: 24783223]

[27]. DeLeon-Pennell KY, de Castro Bras LE, Iyer RP, Bratton DR, Jin YF, Ripplinger CM, Lindsey ML, P. gingivalis lipopolysaccharide intensifies inflammation post-myocardial infarction through matrix metalloproteinase-9, J. Mol. Cell. Cardiol 76 (2014) 218–226. [PubMed: 25240641]

[28]. Deleon-Pennell KY, de Castro Brás LE, Lindsey ML, Circulating porphyromonas gingivalis lipopolysaccharide resets cardiac homeostasis in mice through a matrix metalloproteinase-9-dependent mechanism, Physiol. Rep 1 (5) (2013) e00079. [PubMed: 24159380]

[29]. Iyer RP, de Castro Brás LE, Cannon PL, Ma Y, DeLeon-Pennell KY, Jung M, Flynn ER, Henry JB, Bratton DR, White JA, Fulton LK, Grady AW, Lindsey ML, Defining the sham environment for post-myocardial infarction studies in mice, Am. J. Physiol. Heart Circ. Physiol 311 (3) (2016) H822–H836. [PubMed: 27521418]

[30]. Iyer RP, de Castro Brás LE, Patterson NL, Bhowmick M, Flynn ER, Asher M, Cannon PL, Deleon-Pennell KY, Fields GB, Lindsey ML, Early matrix metalloproteinase-9 inhibition post-myocardial infarction worsens cardiac dysfunction by delaying inflammation resolution, J. Mol. Cell. Cardiol 100 (2016) 109–117. [PubMed: 27746126]

[31]. Iyer RP, Patterson NL, Zouein FA, Ma Y, Dive V, de Castro Bras LE, Lindsey ML, Early matrix metalloproteinase-12 inhibition worsens post-myocardial infarction cardiac dysfunction by delaying inflammation resolution, Int. J. Cardiol 185 (2015) 198–208. [PubMed: 25797678]

[32]. Lindsey ML, Iyer RP, Zamilpa R, Yabluchanskiy A, DeLeon-Pennell KY, Hall ME, Kaplan A, Zouein FA, Bratton D, Flynn ER, Cannon PL, Tian Y, Jin YF, Lange RA, Tokmina-Roszyk D, Fields GB, de Castro Brás LE, Novel Collagen A, Matricryptin reduces cardiac dysfunction post-myocardial infarction by promoting scar formation and angiogenesis, J. Am. Coll. Cardiol 66 (12) (2015) 1364–1374. [PubMed: 26383724]

[33]. Lindsey ML, Iyer RP, Zamilpa R, Yabluchanskiy A, DeLeon-Pennell KY, Hall ME, Kaplan A, Zouein FA, Bratton D, Flynn ER, Cannon PL, Tian Y, Jin YF, Lange RA, Tokmina-Roszyk D, Fields GB, de Castro Bras LE, A Novel Collagen Matricryptin reduces left ventricular dilation post-myocardial infarction by promoting scar formation and angiogenesis, J. Am. Coll. Cardiol 66 (12) (2015) 1364–1374. [PubMed: 26383724]

[34]. Lindsey ML, Gray GA, Wood SK, Curran-Everett D, Statistical considerations in reporting cardiovascular research, Am. J. Phys. Heart Circ. Phys 315 (2) (2018) H303–H313.

[35]. Yuan R, Peters LL, Paigen B, Mice as a mammalian model for research on the genetics of aging, ILAR J. 52 (1) (2011) 4–15. [PubMed: 21411853]

[36]. Xing S, Tsaih SW, Yuan R, Svenson KL, Jorgenson LM, So M, Paigen BJ, Korstanje R, Genetic influence on electrocardiogram time intervals and heart rate in aging mice, Am. J. Physiol. Heart Circ. Physiol 296 (6) (2009) H1907–H1913. [PubMed: 19395551]

[37]. Yuan R, Tsaih SW, Petkova SB, Marin de Evsikova C, Xing S, Marion MA, Bogue MA, Mills KD, Peters LL, Bult CJ, Rosen CJ, Sundberg JP, Harrison DE, Churchill GA, Paigen B, Aging in inbred strains of mice: study design and interim report on median lifespans and circulating IGF1 levels, Aging Cell 8 (3) (2009) 277–287. [PubMed: 19627267]

[38]. Merentie M, Lipponen JA, Hedman M, Hedman A, Hartikainen J, Huusko J, Lottonen-Raikaslehto L, Parviainen V, Laidinen S, Karjalainen PA, Yla-Herttuala S, Mouse ECG findings in aging, with conduction system affecting drugs and in cardiac pathologies: development and validation of ECG analysis algorithm in mice, Physiol. Rep 3 (12) (2015).

[39]. Ackert-Bicknell CL, Anderson LC, Sheehan S, Hill WG, Chang B, Churchill GA, Chesler EJ, Korstanje R, Peters LL, Aging research using mouse models, Curr. Protoc. Mouse Biol 5 (2) (2015) 95–133. [PubMed: 26069080]

[40]. Hagdorn QAJ, Bossers GPL, Koop A-MC, Piek A, Eijgenraam TR, Feen DEVD, Silljé HHW, Boer RAD, Berger RMF, A novel method optimizing the normalization of cardiac parameters in small animal models: the importance of dimensional indexing, Am. J. Phys. Heart Circ. Phys 316 (6) (2019) H1552–H1557.

[41]. Roe AT, Sjaastad I, Louch WE, Heart failure with preserved ejection fraction, Tidsskrift for den Norske laegeforening 137 (18) (2017).

[42]. Klein FJ, Bell S, Runte KE, Lobel R, Ashikaga T, Lerman LO, LeWinter MM, Meyer M, Heart rate-induced modifications of concentric left ventricular hypertrophy: exploration of a novel therapeutic concept, Am. J. Physiol. Heart Circ. Physiol 311 (4) (2016) H1031–h1039. [PubMed: 27591220]

[43]. Cain PA, Ahl R, Hedstrom E, Ugander M, Allansdotter-Johnsson A, Friberg P, Arheden H, Age and gender specific normal values of left ventricular mass, volume and function for gradient echo magnetic resonance imaging: a cross sectional study, BMC Med. Imaging 9 (1) (2009) 2. [PubMed: 19159437]

[44]. Cieslik KA, Taffet GE, Carlson S, Hermosillo J, Trial J, Entman ML, Immuneinflammatory dysregulation modulates the incidence of progressive fibrosis and diastolic stiffness in the aging heart, J. Mol. Cell. Cardiol 50 (1) (2011) 248–256. [PubMed: 20974150]

[45]. Chiao YA, Rabinovitch PS, The aging heart, Cold Spring Harb Perspect. Med 5 (9) (2015) a025148. [PubMed: 26328932]

[46]. Taffet GE, Pham TT, Hartley CJ, The age-associated alterations in late diastolic function in mice are improved by caloric restriction, J. Gerontol. A Biol. Sci. Med. Sci 52 (6) (1997) B285–B290. [PubMed: 9402929]

[47]. Lim CC, Liao R, Varma N, Apstein CS, Impaired lusitropy-frequency in the aging mouse: role of Ca(2+)-handling proteins and effects of isoproterenol, Am. J. Phys 277 (5) (1999) H2083–H2090.

[48]. Burlew BS, Weber KT, Cardiac fibrosis as a cause of diastolic dysfunction, Herz 27 (2) (2002) 92–98. [PubMed: 12025467]

[49]. Rozenberg S, Tavernier B, Riou B, Swynghedauw B, Page CL, Boucher F, Leiris J, Besse S, Severe impairment of ventricular compliance accounts for advanced age-associated hemodynamic dysfunction in rats, Exp. Gerontol 41 (3) (2006) 289–295. [PubMed: 16413724]

[50]. Diaz Brinton R, Minireview: translational animal models of human menopause: challenges and emerging opportunities, Endocrinology 153 (8) (2012) 3571–3578. [PubMed: 22778227]

[51]. Mobbs CV, Gee DM, Finch CE, Reproductive senescence in female C57BL/6J mice: ovarian impairments and neuroendocrine impairments that are partially reversible and delayable by ovariectomy, Endocrinology 115 (5) (1984) 1653–1662. [PubMed: 6541567]

[52]. Bellino FL, Nonprimate animal models of menopause: workshop report, Menopause (New York, N.Y.) 7 (1) (2000) 14–24. [PubMed: 10646699]

[53]. Kerkhof PLM, Kuznetsova T, Ali R, Handly N, Left ventricular volume analysis as a basic tool to describe cardiac function, Adv. Physiol. Educ 42 (1) (2018) 130–139. [PubMed: 29446315]

[54]. Boyle AJ, Shih H, Hwang J, Ye J, Lee B, Zhang Y, Kwon D, Jun K, Zheng D, Sievers R, Angeli F, Yeghiazarians Y, Lee R, Cardiomyopathy of aging in the mammalian heart is characterized by myocardial hypertrophy, fibrosis and a predisposition towards cardiomyocyte apoptosis and autophagy, Exp. Gerontol 46 (7) (2011) 549–559. [PubMed: 21377520]

[55]. Koch SE, Haworth KJ, Robbins N, Smith MA, Lather N, Anjak A, Jiang M, Varma P, Jones WK, Rubinstein J, Age- and gender-related changes in ventricular performance in wild-type FVB/n mice as evaluated by conventional and vector velocity echocardiography imaging: a retrospective study, Ultrasound Med. Biol 39 (11) (2013) 2034–2043. [PubMed: 23791351]

[56]. Olsson MC, Palmer BM, Leinwand LA, Moore RL, Gender and aging in a transgenic mouse model of hypertrophic cardiomyopathy, Am. J. Physiol. Heart Circ. Physiol 280 (3) (2001) H1136–H1144. [PubMed: 11179057]

[57]. Scherrer-Crosbie M, Kurtz B, Ventricular remodeling and function: insights using murine echocardiography, J. Mol. Cell. Cardiol 48 (3) (2010) 512–517. [PubMed: 19615377]

[58]. Dai DF, Rabinovitch PS, Cardiac aging in mice and humans: the role of mitochondrial oxidative stress, Trends Cardiovasc. Med 19 (7) (2009) 213–220. [PubMed: 20382344]

[59]. Dai DF, Santana LF, Vermulst M, Tomazela DM, Emond MJ, MacCoss MJ, Gollahon K, Martin GM, Loeb LA, Ladiges WC, Rabinovitch PS, Overexpression of catalase targeted to mitochondria attenuates murine cardiac aging, Circulation 119 (21) (2009) 2789–2797. [PubMed: 19451351]

[60]. Keller KM, Howlett SE, Sex differences in the biology and pathology of the aging heart, Can. J. Cardiol 32 (9) (2016) 1065–1073. [PubMed: 27395082]

[61]. Olivetti G, Melissari M, Capasso JM, Anversa P, Cardiomyopathy of the aging human heart. Myocyte loss and reactive cellular hypertrophy, Circ. Res 68 (6) (1991) 1560–1568. [PubMed: 2036710]

[62]. Olivetti G, Giordano G, Corradi D, Melissari M, Lagrasta C, Gambert SR, Anversa P, Gender differences and aging: effects on the human heart, J. Am. Coll. Cardiol 26 (4) (1995) 1068–1079. [PubMed: 7560601]

[63]. Shepherd DL, Nichols CE, Croston TL, McLaughlin SL, Petrone AB, Lewis SE, Thapa D, Long DM, Dick GM, Hollander JM, Early detection of cardiac dysfunction in the type 1 diabetic heart

using speckle-tracking based strain imaging, J. Mol. Cell. Cardiol 90 (2016) 74–83. [PubMed: 26654913]

[64]. Potter E, Marwick TH, Assessment of left ventricular function by echocardiography: the case for routinely adding global longitudinal strain to ejection fraction, J. Am. Coll. Cardiol. Img 11 (2 Pt 1) (2018) 260–274.

[65]. Shah AM, Claggett B, Sweitzer NK, Shah SJ, Anand IS, Liu L, Pitt B, Pfeffer MA, Solomon SD, Prognostic importance of impaired systolic function in heart failure with preserved ejection fraction and the impact of spironolactone, Circulation 132 (5) (2015) 402–414. [PubMed: 26130119]

[66]. Kupari M, Laine M, Turto H, Lommi J, Werkkala K, Circulating collagen metabolites, myocardial fibrosis and heart failure in aortic valve stenosis, J. Heart Valve Dis 22 (2) (2013) 166–176. [PubMed: 23798204]

[67]. Hough C, Radu M, Dore JJ, Tgf-beta induced Erk phosphorylation of smad linker region regulates smad signaling, PLoS One 7 (8) (2012) e42513. [PubMed: 22880011]

[68]. Hayashida T, Decaestecker M, Schnaper HW, Cross-talk between ERK MAP kinase and Smad signaling pathways enhances TGF-beta-dependent responses in human mesangial cells, FASEB J. 17 (11) (2003) 1576–1578. [PubMed: 12824291]

[69]. Engel ME, McDonnell MA, Law BK, Moses HL, Interdependent SMAD and JNK signaling in transforming growth factor-beta-mediated transcription, J. Biol. Chem 274 (52) (1999) 37413–37420. [PubMed: 10601313]

[70]. Mori S, Matsuzaki K, Yoshida K, Furukawa F, Tahashi Y, Yamagata H, Sekimoto G, Seki T, Matsui H, Nishizawa M, Fujisawa J, Okazaki K, TGF-beta and HGF transmit the signals through JNK-dependent Smad2/3 phosphorylation at the linker regions, Oncogene 23 (44) (2004) 7416–7429. [PubMed: 15326485]

[71]. Zhang G, Ezura Y, Chervoneva I, Robinson PS, Beason DP, Carine ET, Soslowsky LJ, Iozzo RV, Birk DE, Decorin regulates assembly of collagen fibrils and acquisition of biomechanical properties during tendon development, J. Cell. Biochem 98 (6) (2006) 1436–1449. [PubMed: 16518859]

[72]. Reed CC, Iozzo RV, The role of decorin in collagen fibrillogenesis and skin homeostasis, Glycoconj. J 19 (4–5) (2002) 249–255. [PubMed: 12975602]

[73]. Zhao S, Wu H, Xia W, Chen X, Zhu S, Zhang S, Shao Y, Ma W, Yang D, Zhang J, Periostin expression is upregulated and associated with myocardial fibrosis in human failing hearts, J. Cardiol 63 (5) (2014) 373–378. [PubMed: 24219836]

[74]. Li Q, Liu X, Wei J, Ageing related periostin expression increase from cardiac fibroblasts promotes cardiomyocytes senescent, Biochem. Biophys. Res. Commun 452 (3) (2014) 497–502. [PubMed: 25173938]

[75]. Graf K, Stawowy P, Osteopontin: a protective mediator of cardiac fibrosis? Hypertension 44 (6) (2004) 809–810. [PubMed: 15520299]

[76]. O'Regan A, Berman JS, Osteopontin: a key cytokine in cell-mediated and granulomatous inflammation, Int. J. Exp. Pathol 81 (6) (2000) 373–390. [PubMed: 11298186]

[77]. O'Brien ER, Garvin MR, Stewart DK, Hinohara T, Simpson JB, Schwartz SM, Giachelli CM, Osteopontin is synthesized by macrophage, smooth muscle, and endothelial cells in primary and restenotic human coronary atherosclerotic plaques, Arterioscler. Thromb 14 (10) (1994) 1648–1656. [PubMed: 7918316]

[78]. Mazzali M, Kipari T, Ophascharoensuk V, Wesson JA, Johnson R, Hughes J, Osteopontin—a molecule for all seasons, QJM 95 (1) (2002) 3–13. [PubMed: 11834767]

[79]. Tamura A, Shingai M, Aso N, Hazuku T, Nasu M, Osteopontin is released from the heart into the coronary circulation in patients with a previous anterior wall myocardial infarction, Circ. J 67 (9) (2003) 742–744. [PubMed: 12939547]

[80]. Szalay G, Sauter M, Haberland M, Zuegel U, Steinmeyer A, Kandolf R, Klingel K, Osteopontin: a fibrosis-related marker molecule in cardiac remodeling of enterovirus myocarditis in the susceptible host, Circ. Res 104 (7) (2009) 851–859. [PubMed: 19246678]

[81]. López B, González A, Lindner D, Westermann D, Ravassa S, Beaumont J, Gallego I, Zudaire A, Brugnolaro C, Querejeta R, Larman M, Tschöpe C, Díez J, Osteopontin-mediated myocardial

fibrosis in heart failure: a role for lysyl oxidase? Cardiovasc. Res 99 (1) (2013) 111–120. [PubMed: 23619422]

[82]. Itoh Y, Discoidin domain receptors: microenvironment sensors that promote cellular migration and invasion, Cell Adhes. Migr (2018) 1–8.

[83]. Hou G, Vogel WF, Bendeck MP, Tyrosine kinase activity of discoidin domain receptor 1 is necessary for smooth muscle cell migration and matrix metalloproteinase expression, Circ. Res 90 (11) (2002) 1147–1149. [PubMed: 12065315]

[84]. Ram R, Lorente G, Nikolich K, Urfer R, Foehr E, Nagavarapu U, Discoidin domain receptor-1a (DDR1a) promotes glioma cell invasion and adhesion in association with matrix metalloproteinase-2, J. Neuro-Oncol 76 (3) (2006) 239–248.

[85]. Song W, Wang H, Wu Q, Atrial natriuretic peptide in cardiovascular biology and disease (NPPA), Gene 569 (1) (2015) 1–6. [PubMed: 26074089]

[86]. Feng JA, Perry G, Mori T, Hayashi T, Oparil S, Chen YF, Pressure-independent enhancement of cardiac hypertrophy in atrial natriuretic peptide-deficient mice, Clin. Exp. Pharmacol. Physiol 30 (5–6) (2003) 343–349. [PubMed: 12859424]

[87]. Knowles JW, Esposito G, Mao L, Hagaman JR, Fox JE, Smithies O, Rockman HA, Maeda N, Pressure-independent enhancement of cardiac hypertrophy in natriuretic peptide receptor A-deficient mice, J. Clin. Invest 107 (8) (2001) 975–984. [PubMed: 11306601]

[88]. Holtwick R, van Eickels M, Skryabin BV, Baba HA, Bubikat A, Begrow F, Schneider MD, Garbers DL, Kuhn M, Pressure-independent cardiac hypertrophy in mice with cardiomyocyte-restricted inactivation of the atrial natriuretic peptide receptor guanylyl cyclase-a, J. Clin. Invest 111 (9) (2003) 1399–1407. [PubMed: 12727932]

[89]. Meschiari CA, Jung M, Iyer RP, Yabluchanskiy A, Toba H, Garrett MR, Lindsey ML, Macrophage overexpression of matrix metalloproteinase-9 in aged mice improves diastolic physiology and cardiac wound healing after myocardial infarction, Am. J. Physiol. Heart Circ. Physiol 314 (2) (2018) H224–H235. [PubMed: 29030341]

[90]. Medrano G, Hermosillo-Rodriguez J, Pham T, Granillo A, Hartley CJ, Reddy A, Osuna PM, Entman ML, Taffet GE, Left atrial volume and pulmonary artery diameter are noninvasive measures of age-related diastolic dysfunction in mice, J. Gerontol. A Biol. Sci. Med. Sci 71 (9) (2016) 1141–1150. [PubMed: 26511013]

[91]. Feridooni HA, Kane AE, Ayaz O, Boroumandi A, Polidovitch N, Tsushima RG, Rose RA, Howlett SE, The impact of age and frailty on ventricular structure and function in C57BL/6J mice, J. Physiol 595 (12) (2017) 3721–3742. [PubMed: 28502095]

[92]. Sheng Y, Lv S, Huang M, Lv Y, Yu J, Liu J, Tang T, Qi H, Di W, Ding G, Opposing effects on cardiac function by calorie restriction in different-aged mice, Aging Cell 16 (5) (2017) 1155–1167. [PubMed: 28799249]

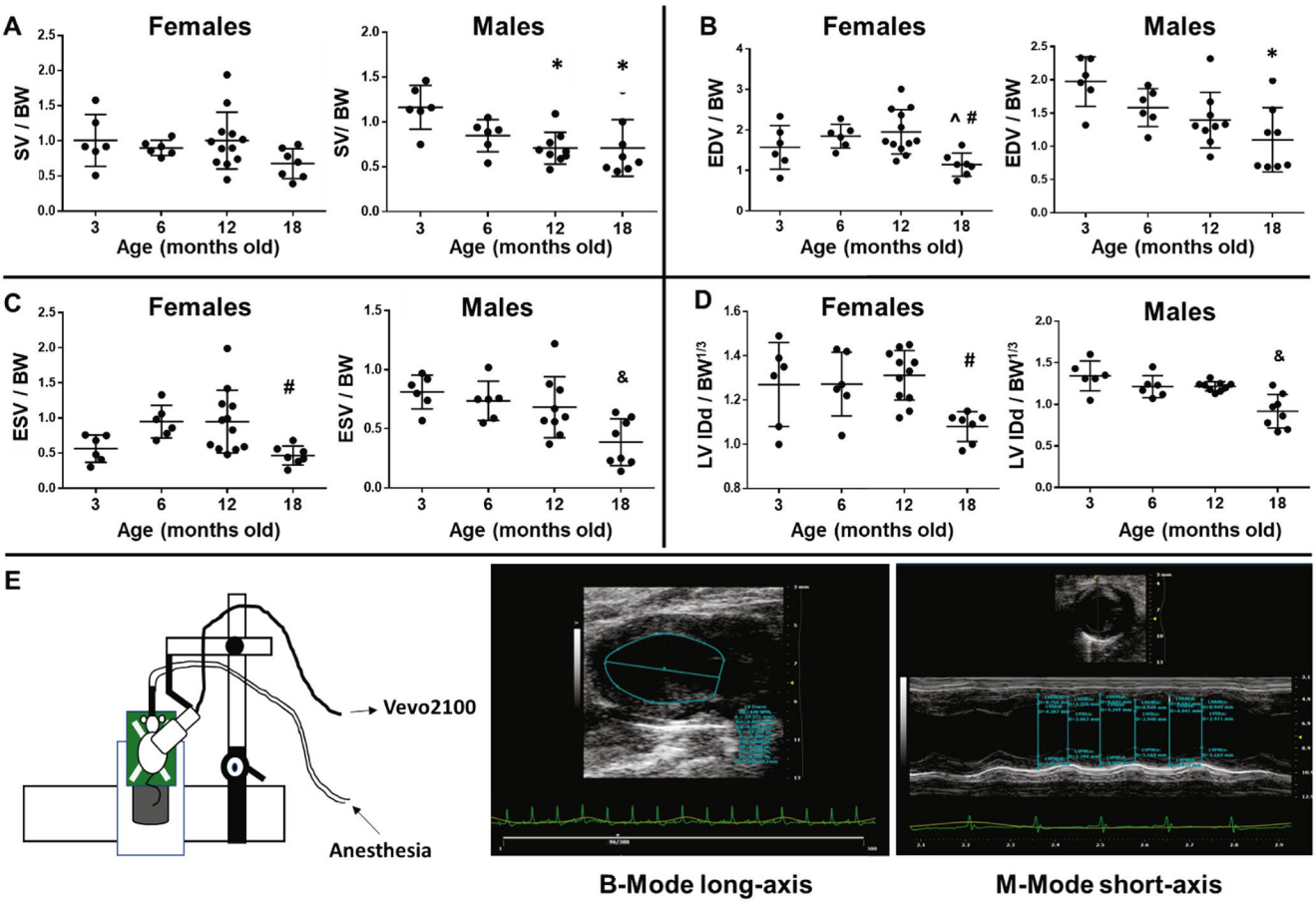

Fig. 1.

Sex-dependent cardiac dysfunction. A) Age-dependent stroke volume (SV) changes were observed only in males. B) Males show a trend for earlier concentric remodeling in old animals showing reduced end-diastolic volume (EDV) compared to young adults. C) and D) Old females displayed reduced ESV and internal diameter at diastole (IDd) compared only to middle-age while old males presented reduced ESV and IDd versus all other ages. E) Diagram depicting probe position during long-axis acquisition (left panel), the probe was rotated 90 degrees to acquire short-axis images; middle-panel displays representative image of a B-mode long-axis with LV trace; and right panel shows a representative image of M-Mode short axis with measurements of wall thicknesses and LV diameter. *$p < .05$ versus 3 m.o., ^p < .05 versus 6 m.o., #p < .05 versus 12 m.o., &p < .05 versus all other age groups, $n = 6–12$/age.

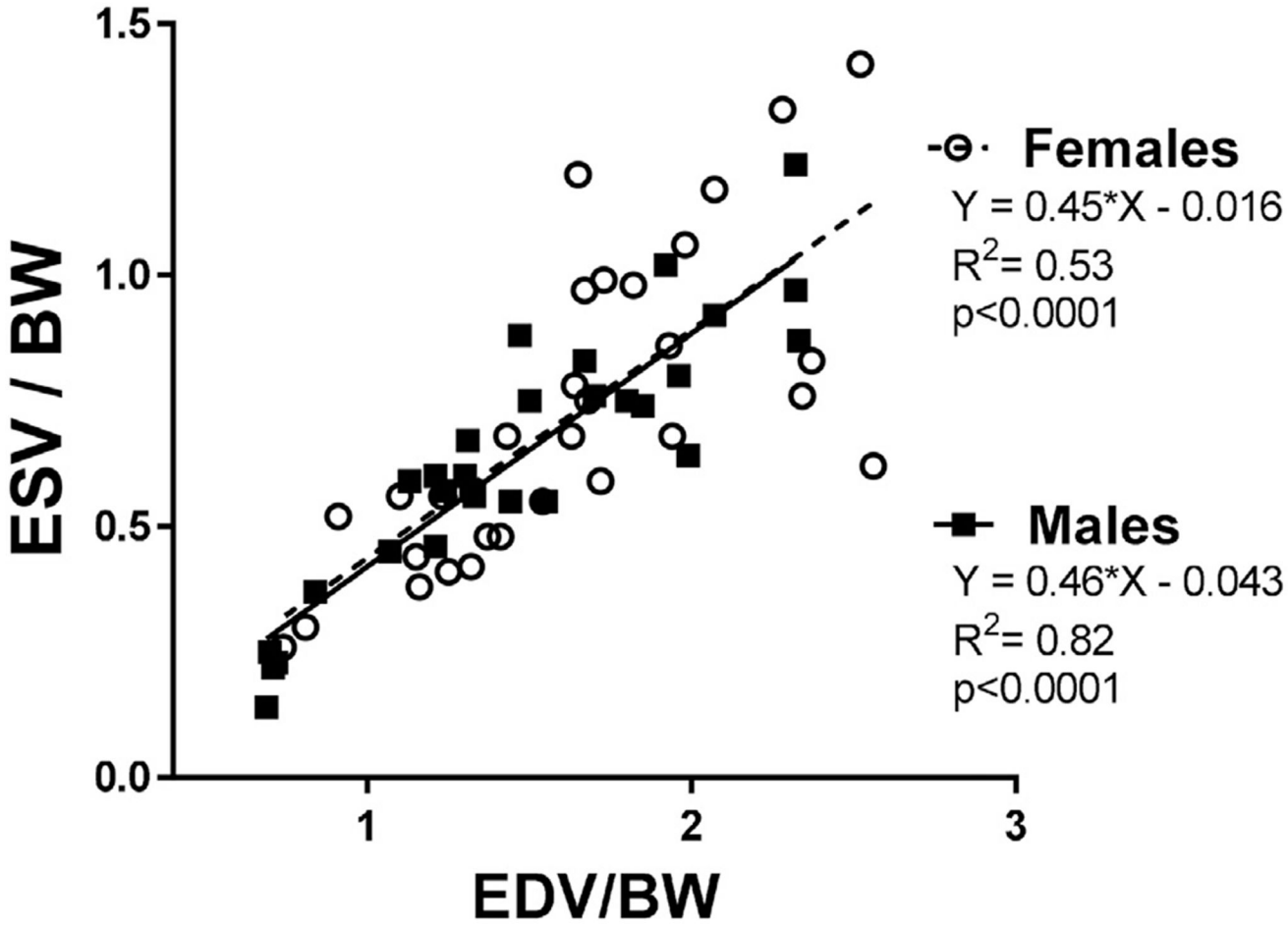

Fig. 2.
EDV and ESV linear regression, stratified by sex.

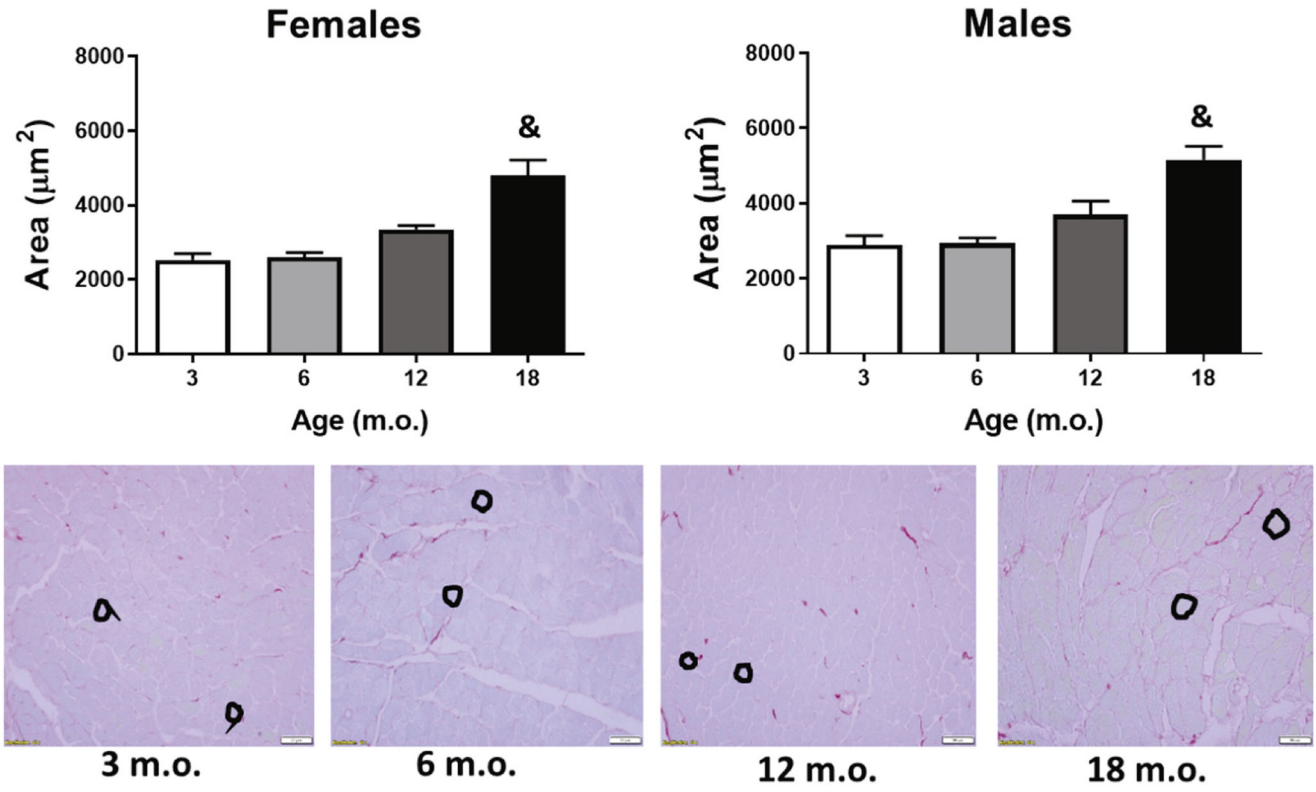

Fig. 3.

Cardiomyoctye cross-sectional area. Old mice presented cardiomyocyte hypertrophy compared to all younger groups. Black circles are representative traces of cross-sections in cardiomyocytes. &$p < .05$ versus all other groups. $n = 6$/sex/age.

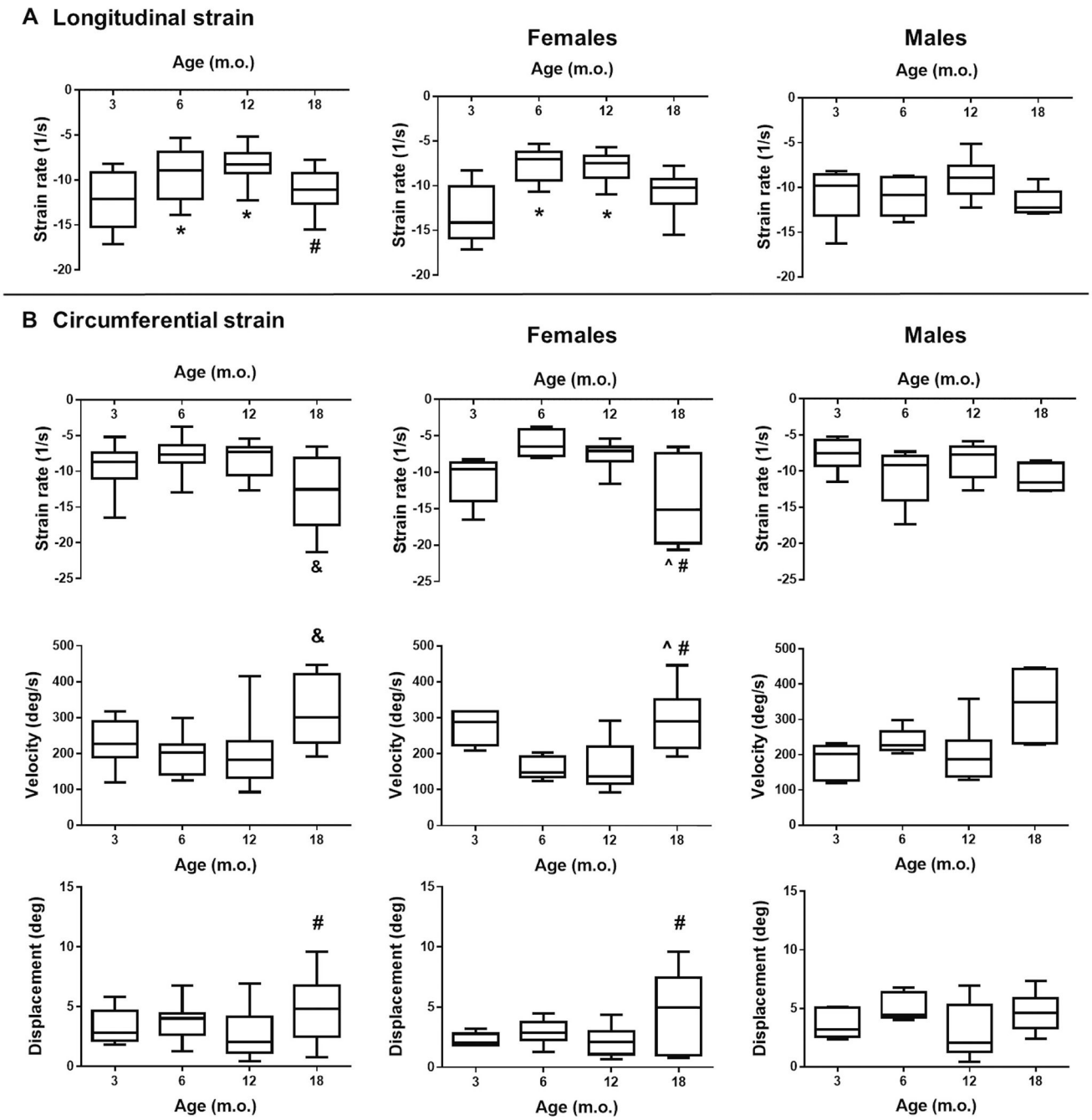

Fig. 4.

STE measurements. A) Longitudinal strain analysis (long-axis). B) Circumferential strain analysis (short-axis). Left panels: Both sexes; Middle-panels: Females; Right panels: Males; **p* < .05 versus 3 m.o., ^p < .05 versus 6 m.o., #p < .05 versus 12 m.o., & p < .05 versus all other age groups, *n* = 12–18/group (males and females).

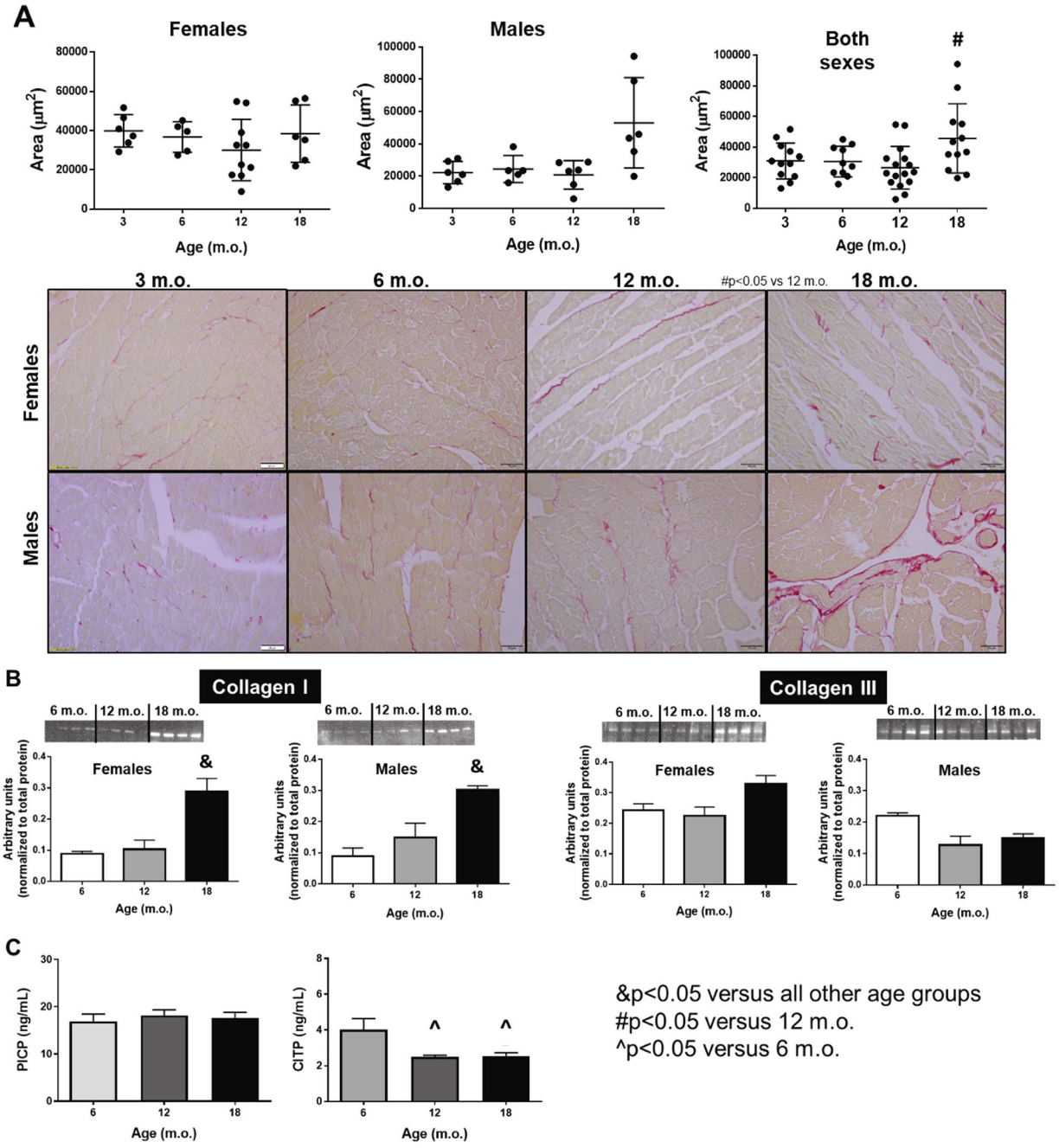

Fig. 5.

Interstitial collagen deposition increases with age in a sex-independent manner. A) Histological quantification of interstitial collagen deposition quantified by picro sirius red staining. B) Collagen type I and III protein expression measured by immunoblot. C) Plasma levels of PICP (collagen synthesis) and CITP (collagen degradation). n = 6/sex/age. (For interpretation of the references to colour in this figure legend, the reader is referred to the web version of this article.)

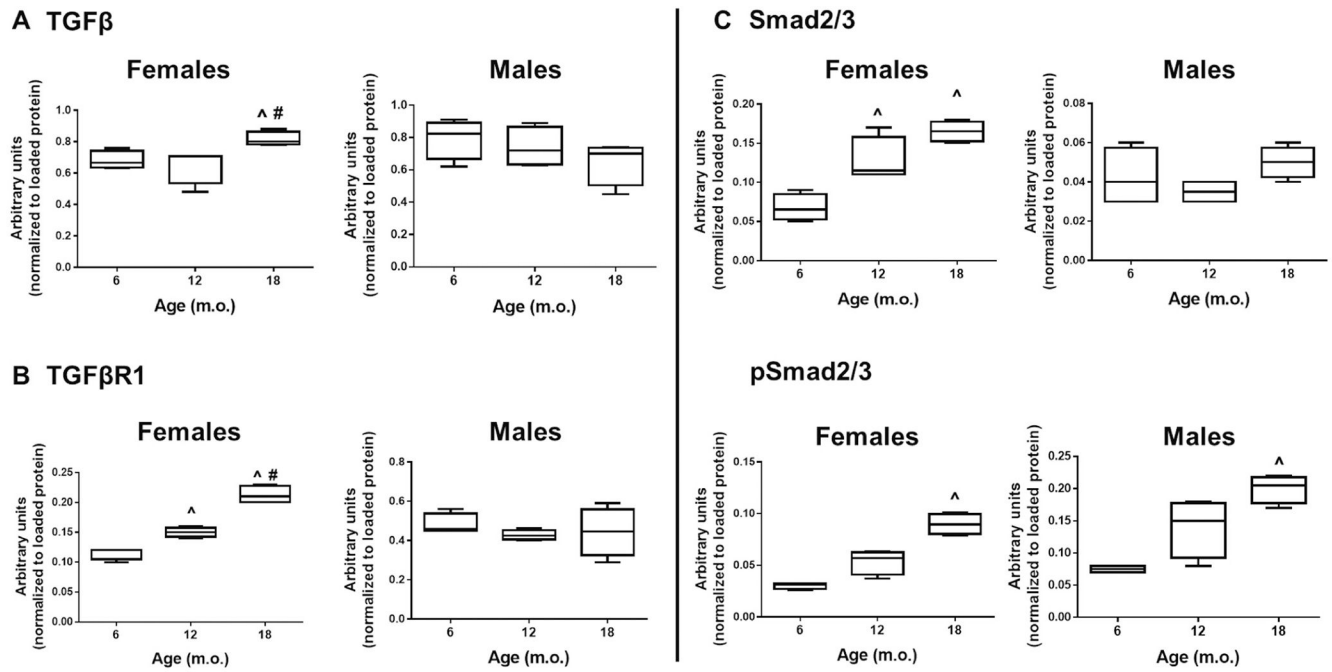

Fig. 6.

The TGFβ pathway was mostly affected in females, with increased signaling in the old mice compared to younger ages. ^$p < .05$ versus 6 m.o., #$p < .05$ versus 12 m.o., $n = 4$/group.

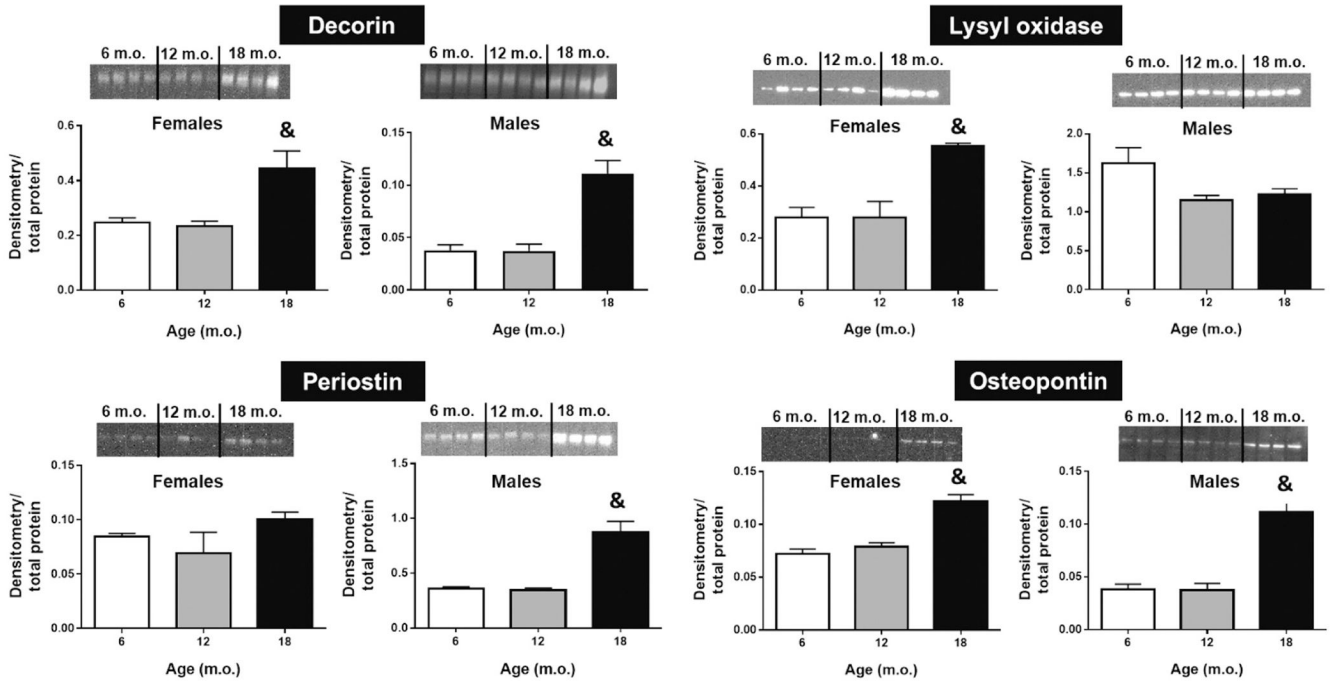

Fig. 7.

ECM related proteins and proteoglycans with age. Decorin and osteopontin levels are increased at 18 m.o compared to younger groups and this is not dependent on sex. Lysyl oxidase was only observed at higher levels in old females, while periostin was augmented in old males. Quantification by densitometry was normalized to total protein (loaded protein) for each lane; $n = 4–6$/group. &$p < .05$ versus all groups.

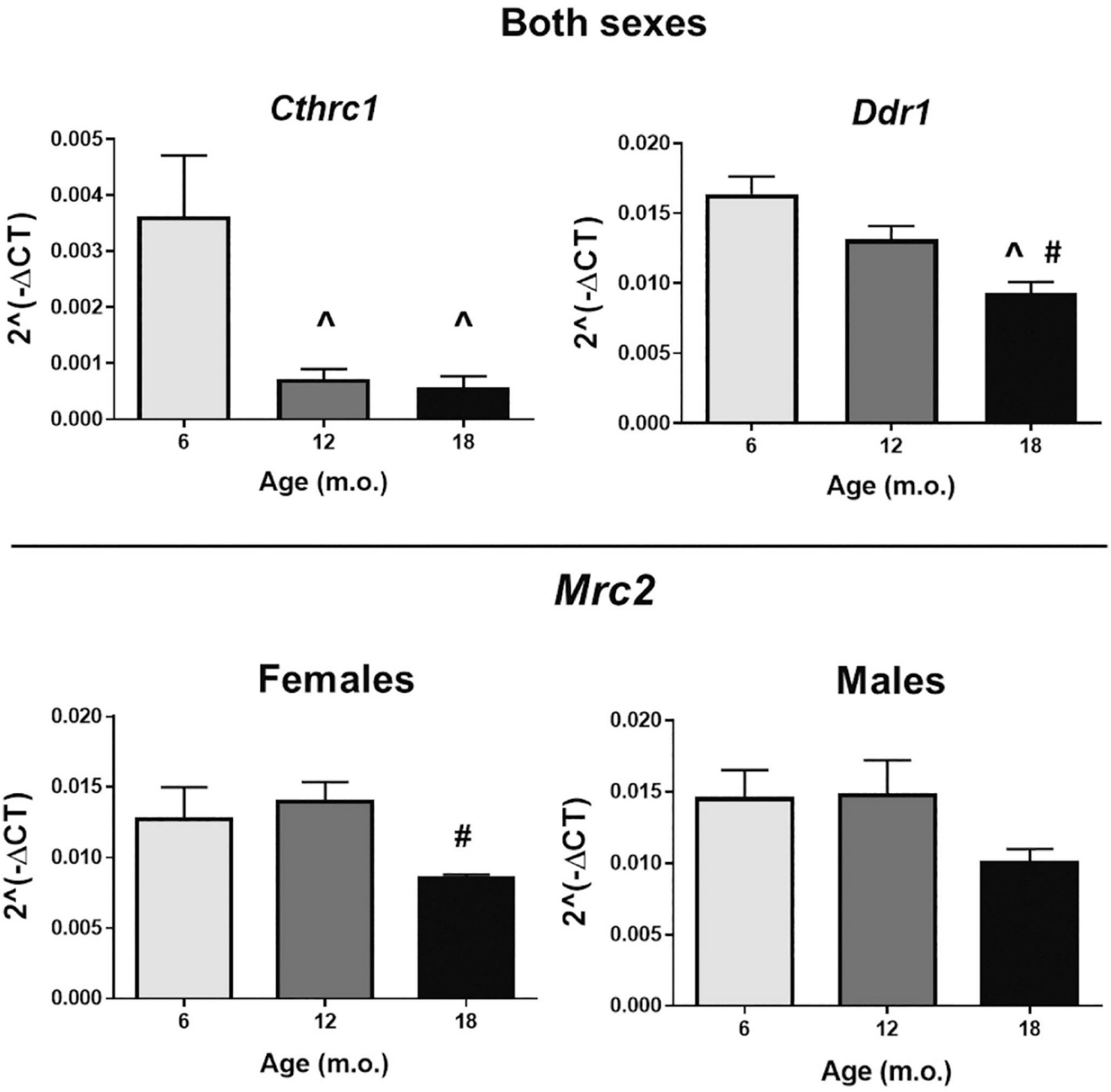

Fig. 8.

Negative regulators of collagen deposition, such as collagen triple helix repeat-containing protein 1 (Cthrc1), discoidin domain receptor 1 (Ddr1), and C-type mannose receptor-2 (Mrc2) were all reduced with age. However, Mrc2 changes were driven by females only, n = 8/group. ^p < .05 versus 6 m.o.; #p < .05 versus 12 m.o.

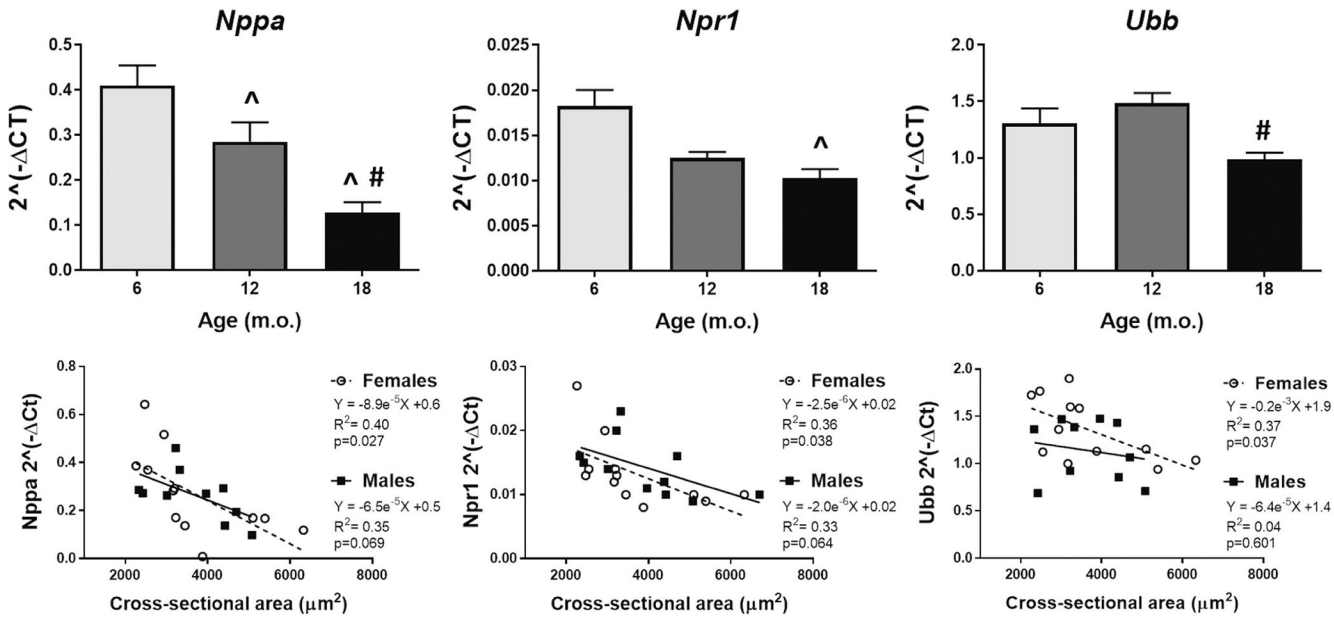

Fig. 9.

Cardiac homeostasis is lost with age and in females this correlates with cardiomyocyte hypertrophy. Left panel: natriuretic peptide A; middle-panel: atrial natriuretic peptide receptor 1; and right panel: ubiquitin B. ^p < .05 versus 6 m.o., #p < .05 versus 12 m.o. *n* = 8/group (4 males and 4 females).

Health Research Alliance Author Manuscript

Table 1

Echocardiographic (conventional) parameters normalized to BW or $BW^{1/3}$. Values are mean ± standard deviation.

Ages	Females				Males				Both sexes			
	3 m.o.	6 m.o.	12 m.o.	18 m.o.	3 m.o.	6 m.o.	12 m.o.	18 m.o.	3 m.o.	6 m.o.	12 m.o.	18 m.o.
Body weight (g)	20 ± 2	28 ± 3	32 ± 5 *	45 ± 10 *	26 ± 4	32 ± 6	48 ± 7 $^{*\wedge}$	39 ± 8 $^{*\#}$	23 ± 4	30 ± 5 *	39 ± 10 $^{*\wedge}$	42 ± 9 $^{*\wedge}$
LV Mass wet weight (mg)	83 ± 19	97 ± 7.0	115 ± 22 *	103 ± 13	91 ± 9	113 ± 17	123 ± 24 *	110 ± 17	87 ± 15	105 ± 15 *	118 ± 23 *	107 ± 15 *
Heart Rate (BPM)	411 ± 20	419 ± 33	419 ± 27	448 ± 42	407 ± 9	421 ± 22	436 ± 23	471 ± 91	409 ± 15	420 ± 27	426 ± 26	460 ± 71
EDV (µl)/ BW	1.6 ± 0.5	1.8 ± 0.3	2.0 ± 0.5	1.1 ± 0.3 $^{\wedge\#}$	2.0 ± 0.4	1.6 ± 0.3	1.4 ± 0.4	1.1 ± 0.5 *	1.8 ± 0.5	1.7 ± 0.3	1.7 ± 0.6	1.1 ± 0.4 $^{\&}$
ESV (µl)/ BW	0.6 ± 0.2	0.9 ± 0.2	0.9 ± 0.4	0.5 ± 0.1 $^{\#}$	0.8 ± 0.1	0.7 ± 0.2	0.7 ± 0.3	0.4 ± 0.2 $^{\&}$	0.7 ± 0.2	0.8 ± 0.2	0.8 ± 0.3	0.4 ± 0.2 $^{\&}$
SV (µL)/BW	1.0 ± 0.4	0.9 ± 0.1	1.0 ± 0.4	0.7 ± 0.2	1.1 ± 0.2	0.8 ± 0.2	0.7 ± 0.2 *	0.7 ± 0.3 *	1.1 ± 0.3	0.9 ± 0.1	0.8 ± 0.3 *	0.7 ± 0.3 *
EF (%, normalized volumes)	64 ± 5.0	49 ± 5.0	52 ± 15	59 ± 10.0	59 ± 3.0	53 ± 6.0	52 ± 6.0	66 ± 8.0 $^{\wedge\#}$	61 ± 5.0	51 ± 6.0 *	52 ± 12.0	62 ± 9 $^{\wedge\#}$
$LVAWd/BW^{1/3}$	0.3 ± 0.0	0.3 ± 0.0	0.3 ± 0.0	0.3 ± 0.1	0.3 ± 0.0	0.3 ± 0.1	0.3 ± 0.0	0.3 ± 0.1	0.3 ± 0.0	0.3 ± 0.0	0.3 ± 0.0	0.3 ± 0.1
$LVAWs/BW^{1/3}$	0.3 ± 0.0	0.3 ± 0.0	0.3 ± 0.1	0.4 ± 0.1	0.4 ± 0.0	0.3 ± 0.1	0.3 ± 0.0	0.4 ± 0.1	0.3 ± 0.0	0.3 ± 0.1	0.3 ± 0.1	0.4 ± 0.1
$LVIDd (mm)/BW^{1/3}$	1.3 ± 0.2	1.3 ± 0.1	1.3 ± 0.1	1.1 ± 0.1 $^{\#}$	1.3 ± 0.2	1.2 ± 0.1	1.2 ± 0.1	0.9 ± 0.2 $^{\&}$	1.3 ± 0.2	1.2 ± 0.1	1.3 ± 0.1	1.0 ± 0.2 $^{\&}$
$LVIDs (mm)/BW^{1/3}$	0.8 ± 0.1	1.0 ± 0.1	0.9 ± 0.1	0.7 ± 0.1 $^{\wedge\#}$	0.9 ± 0.1	0.8 ± 0.2	0.9 ± 0.1	0.5 ± 0.2 $^{\&}$	0.8 ± 0.1	0.9 ± 0.2	0.9 ± 0.1	0.6 ± 0.2 $^{\&}$
$LVPWd (mm)/BW^{1/3}$	0.3 ± 0.0	0.2 ± 0.0	0.3 ± 0.0	0.3 ± 0.0	0.2 ± 0.0	0.3 ± 0.0	0.3 ± 0.0	0.3 ± 0.1	0.3 ± 0.0	0.2 ± 0.0	0.3 ± 0.0	0.3 ± 0.1
$LVPWs (mm)/BW^{1/3}$	0.4 ± 0.1	0.4 ± 0.1	0.4 ± 0.1	0.4 ± 0.1	0.4 ± 0.1	0.4 ± 0.1	0.3 ± 0.1	0.4 ± 0.1	0.4 ± 0.1	0.4 ± 0.1	0.3 ± 0.1	0.4 ± 0.1 $^{\#}$
FS (%, normalized dimensions)	41 ± 4.0	25 ± 5.0 *	30 ± 8.0 *	36 ± 9.0	35 ± 7.0	33 ± 10.0	26 ± 6.0	43 ± 13.0 $^{\#}$	38 ± 6.0	29 ± 9.0	28 ± 8.0 *	40 ± 12.0 $^{\wedge\#}$
Cardiac output (mL/min)/BW	0.4 ± 0.1	0.4 ± 0.0	0.4 ± 0.2	0.3 ± 0.1	0.5 ± 0.1	0.4 ± 0.1	0.3 ± 0.1	2.9 ± 1.4 $^{\&}$	0.4 ± 0.1	0.4 ± 0.1	0.4 ± 0.1	1.7 ± 1.7 $^{\&}$

* $p < .05$ versus 3 m.o.,

$^{\wedge}$ $p < .05$ versus 6 m.o.,

$^{\#}$ $p < .05$ versus 12 m.o.,

$^{\&}$ $p < .05$ versus all other age groups.